

Protein Phosphatase 2A (PP2A) Regulates Low Density Lipoprotein Uptake through Regulating Sterol Response Element-binding Protein-2 (SREBP-2) DNA Binding*

Received for publication, April 1, 2014, and in revised form, April 25, 2014. Published, JBC Papers in Press, April 26, 2014, DOI 10.1074/jbc.M114.570390

Lyndi M. Rice^{†1}, Melissa Donigan^{§1}, Muhua Yang[§], Weidong Liu[§], Devanshi Pandya[§], Biny K. Joseph[§], Valerie Sodi[‡], Tricia L. Gearhart[¶], Jenny Yip[§], Michael Bouchard[¶], and Joseph T. Nickels, Jr.^{§2}

From the [‡]Oncoveda Cancer Institute and the [§]Institute of Metabolic Disorders, Genesis Biotechnology Group, Hamilton, New Jersey 08691 and the [¶]Department of Molecular Biology and Biochemistry, Drexel University College of Medicine, Philadelphia, Pennsylvania 19129

Background: The sterol response element-binding protein-2 (SREBP-2) regulates *LDLR* gene expression.

Results: Protein phosphatase 2A regulates SREBP-2 binding to an *LDLR* promoter SRE.

Conclusion: PP2A regulates LDL uptake.

Significance: A novel pathway regulating LDL uptake has been elucidated.

LDL-cholesterol (LDL-C) uptake by *Ldlr* is regulated at the transcriptional level by the cleavage-dependent activation of membrane-associated sterol response element-binding protein (SREBP-2). Activated SREBP-2 translocates to the nucleus, where it binds to an *LDLR* promoter sterol response element (SRE), increasing *LDLR* gene expression and LDL-C uptake. SREBP-2 cleavage and translocation steps are well established. Several SREBP-2 phosphorylation sites have been mapped and functionally characterized. The phosphatases dephosphorylating these sites remain elusive. The phosphatase(s) regulating SREBP-2 represents a novel pharmacological target for treating hypercholesterolemia. Here we show that protein phosphatase 2A (PP2A) promotes SREBP-2 *LDLR* promoter binding in response to cholesterol depletion. No binding to an *LDLR* SRE was observed in the presence of the HMG-CoA reductase inhibitor, lovastatin, when PP2A activity was inhibited by okadaic acid or depleted by siRNA methods. SREBP-2 cleavage and nuclear translocation were not affected by loss of PP2A. PP2A activity was required for SREBP-2 DNA binding. In response to cholesterol depletion, PP2A directly interacted with SREBP-2 and altered its phosphorylation state, causing an increase in SREBP-2 binding to an *LDLR* SRE site. Increased binding resulted in induced *LDLR* gene expression and increased LDL uptake. We conclude that PP2A activity regulates cholesterol homeostasis and LDL-C uptake.

Cholesterol biosynthesis and uptake are important pathways that are required for cell maintenance because cholesterol is an essential lipid and is important for maintaining membrane fluidity, raft formation, and steroid and bile acid syntheses (1–4). Moreover, proper LDL-C³ uptake is essential for maintaining

normal LDL-C blood level. Cholesterol itself is an important second messenger regulating developmental cell signaling (5–7). Deregulation of cholesterol metabolism leads to a chronic increase in blood plasma cholesterol level, which is a major risk factor for cardiovascular disease and atherosclerosis.

Current drug therapies (statins) have targeted *de novo* cholesterol biosynthesis as treatment for cardiovascular disease (8–10). Although statins are able to reduce blood plasma cholesterol levels by inhibiting HMG-CoA reductase (HMGCR), ~10–20% of patients are unable to tolerate treatment and have irrevocable joint pain and, in some cases, liver toxicity (11–15). Moreover, statins have a threshold as far as how low they can reduce LDL-C; thus, ~55–65% of patients still remain at risk for cardiovascular events (16). These patients may go on a higher dose of statin, which in some cases increases the incidence of side effects (17). Thus, novel therapies treating lipid disorders are needed to help statin-intolerant individuals. One such potential biologic therapy that is in clinical trials targets Pcsk9, which is involved in the degradation of *Ldlr* (18).

De novo cholesterol biosynthesis requires the induction of genes regulated by the transcription factor known as SREBP-2, one of three SREBPs encoded by mammalian cells. SREBP-2, along with SREBP-1a, activates genes required for cholesterol biosynthesis and LDL-C uptake, whereas SREBP-1c is important for fatty acid synthesis (19).

SREBP-2 is localized in the ER when cholesterol level is high but is transported to the Golgi and cleaved in response to a decrease in cholesterol sensed by sterol cleavage-activating protein (19). Two cleavage events within the Golgi by site 1 and site 2 protease lead to the generation of a soluble SREBP-2 active fragment transcription factor (SREBP-2*af*) that is transported to the nucleus (20). Nuclear SREBP-2*af* binds SREs in the promoters of genes required for *de novo* cholesterol biosynthesis, resulting in increased gene expression. These include

protein; SREBP-2*af*, SREBP-2 active fragment transcription factor; LDLR, low density lipoprotein receptor; HMGCR, HMG-CoA reductase; OA, okadaic acid; *Csi*, control siRNA; ChREBP, carbohydrate-binding element-binding protein transcription factor; qRT-PCR, quantitative RT-PCR.

* This work was supported by the Genesis Biotechnology Group.

¹ Both authors contributed equally to this work.

² To whom correspondence should be addressed: The Institute of Metabolic Disorders LLC, Genesis Biotechnology Group, 1000 Waterview Dr., Hamilton, NJ 08691. Tel.: 609-786-2870; E-mail: jnickels@venenumbiodesign.com.

³ The abbreviations used are: LDL-C, low density lipoprotein-cholesterol; PP2A, protein phosphatase 2A; SREBP, sterol response element-binding

HMGCR, *HMGS1* (HMG-CoA synthase), *FDFT1* (squalene synthase), and the *LDLR* gene required for LDL-C uptake (21).

PP2A is a heterotrimeric serine/threonine protein phosphatase that regulates many cell events, including cell cycle progression and cell signaling pathways (22). PP2A is composed of a core enzyme dimer consisting of a catalytic subunit (C) and an A structural subunit (22). The AC dimer recruits specific B regulatory subunits that confer substrate specificity and/or determine cell location. Four gene families consisting of several genes, many encoding several isoforms, encode for the B regulatory subunits (23). There are several reports indicating that PP2A regulates lipid-dependent events (24–28). Thus, it seems that PP2A targets multiple factors regulating lipid metabolism, lipid trafficking, and lipid-dependent signaling.

We were interested in identifying novel drug targets to treat cardiovascular disease and atherosclerosis. Here, we uncovered a novel role for PP2A in regulating LDL-C uptake. PP2A is required for SREBP-2-dependent activation of *LDLR* gene expression in response to cholesterol depletion. PP2A directly binds to SREBP-2, altering its phosphorylation status, which causes an enhanced ability to bind an *LDLR* SRE promoter site. Increased binding causes increased *Ldlr* level and increased LDL-C uptake.

EXPERIMENTAL PROCEDURES

Cell Lines, Plasmids, and siRNA Treatment—HepG2 cells were grown in minimum Eagle's medium supplemented with 10% FBS, 1% sodium pyruvate, 1% non-essential amino acids, and 0.1% gentamycin (Invitrogen). THLE-3 cells were grown in BEGM (Clonetics) supplemented with 10% FBS, 5 ng/ml EGF, and 70 ng/ml phosphoethanolamine (Sigma). Rat primary hepatocytes were isolated as described (29). Rats were anesthetized with 60 mg of ketamine/kg of rat and 7.5 mg of xylazine/kg. 50 kilounits/ml of heparin was injected into the femoral vein, and the primary hepatocytes were seeded at a density of 1×10^6 cells in growth medium (Williams E medium supplemented with 1% sodium pyruvate, 2 mM glutamine, 4 μ l/ml ITS medium supplement (1 mg/ml recombinant human insulin; 0.55 mg/ml human transferrin (iron-free), 0.5 μ g/ml sodium selenite), 5 μ g/ml hydrocortisone, 0.01 μ g/ml EGF, and 25 μ g/ml gentamicin). After the initial 3-h incubation, the medium was removed and replaced with growth medium (as above, without gentamycin and with 0.1% DMSO). All cells were plated on collagen-coated plates and were incubated at 37 °C, 5% CO₂. Depending on the statin and cell line used, the concentration of statin ranged from 25 to 75 μ M. 10 nM okadaic acid (OA; Calbiochem) was used for inhibition of PP2A activity. All animal procedures were reviewed and approved by the Drexel University College of Medicine institutional animal care and use committee.

For HepG2 and THLE-3 cells, 100 nM *Csi* or *PPP2Casi* siRNA (Dharmacon) was transfected at 48 and 24 h prior to statin treatment using dharmafect 4 transfection reagent. Cells were then treated with lovastatin (Sigma), atorvastatin, or simvastatin for 24 h. Cells were harvested, washed in $1 \times$ PBS (Invitrogen), and stored at -80 °C until processing. Rat primary hepatocytes were treated with *Csi* or 150 nM *PPP2Casi* siRNA after the initial 3-h incubation and again the next morning,

prior to the addition of 75 μ M lovastatin after 8 h. Cells were harvested 24 h later (30, 31).

The full-length SREBP-2 was cloned into pEGFP-C1 plasmid (Clontech) via XhoI and SacII restriction enzyme sites. The EGFP is linked to the N terminus of SREBP-2. The construct (EGFP-SREBP-2) was confirmed by sequencing.

Lentivirus Production and Overexpression of PP2CA and PPME-1—PP2CA and PPME-1 lentiviral ORF plasmid constructs were obtained from GeneCoeia. To produce ORF lentivirus, 293T packing cells (ATCC) were transfected with second generation packaging plasmids, including *gag*, *pol*, and *rev* (pMDL g/p RRE, RSV-REV, and pVSVG) together with PP2CA-ORF- or PPME-1-ORF-targeting plasmids using Lipofectamine 2000 as indicated (Invitrogen). Lentivirus was harvested and filtered at 24 and 48 h post-transfection.

To infect HepG2-targeting cells, freshly harvested lentivirus was added to virus-containing medium supplemented with hexadimethrine bromide (Polybrene). 48 h postinfection, the cells were subjected to puromycin selection, and the medium was replaced every other day for more than a week. To assay for the infected cells, control and infected cells were either not treated or treated with 50 μ M lovastatin for 5–6 h. The cells were then gently rinsed one time with PBS and pelleted for total RNA extraction.

RNA Extraction and qRT-PCR—RNA was extracted from cells using the RNeasy kit (Qiagen) according to the manufacturer's protocol. 50 ng of RNA was used as a template in the one-step RT-PCR (Quanta) according to the suggested protocol. qRT-PCR was completed on an MxPro 3000 (Stratagene), and data were analyzed using MxPro software. Relative expression was determined by normalizing the expression of all genes of interest to GAPDH expression (ΔCt), and data are represented as -fold change compared with the vehicle-treated sample ($\Delta\Delta Ct$).

The primers used for qRT-PCR were designed using Beacon Designer software and were ordered from IDT. For the HepG2 and THLE-3 human cell lines, the primers used were as follows: GAPDH-FOR, 5'-TGGGCTACACTGAGCACCAG-3'; GAPDH-REV, 5'-GGGTGTCGCTGTTGAAGTCA-3'; LDLR-FOR, 5'-GCTTGTCTGTACCTGCAAA-3'; LDLR-REV, 5'-AACTGCCGAGAGATGCACTT-3'; PPP2CA-FOR, 5'-TGTCCGAGTCCCAGGTCAAG-3'; PPP2CA-REV, 5'-TGCCACCAATTCTAAA-CAGTTCC-3'.

The primer sets used for rat primary hepatocytes were RnGAPDH-FOR (5'-GCAAGTTCAACGGCACAGTCAAG-3'), RnGAPDH-REV (5'-ACATACTCAGCACCAGCATCA-3'), RnLDLR-FOR (5'-AGTGTGAAGATATTGACGAGTG-3'), RnLDLR-REV (5'-ATGGCGTTGGTGAAGAG-3'), RnPPP2CA-FOR (5'-GACTATGTGGACAGAGGATATTAC-3'), and RnPPP2CA-REV (5'-CAAGGCAGTGAGAGGAAGG-3').

Protein Extraction, SDS-PAGE, and Western Analysis—Cells were resuspended in radioimmune precipitation assay buffer and sonicated at 4 °C on ice using the Diagenode Biorupter, for 10 min, using a 30-s on, 30-s off cycle. Cell debris was pelleted by centrifugation for 10 min, and cell lysates were collected and analyzed for protein content using a Bradford assay (Bio-Rad). 50 μ g of whole cell extract was boiled at 100 °C for 10 min and

Regulation of LDL-C Uptake by PP2A

loaded onto a 10% denaturing gel, and proteins were then transferred to 0.45- μ m nitrocellulose (Whatman). Blots were blocked in 5% milk/TBST prior to incubation with primary and secondary antibodies (Amersham Biosciences). Antibodies were detected with the ECL detection kit from Amersham Biosciences. Primary antibodies for SREBP-2, LDLR, FDF1, PPP2CA (protein phosphatase 2A α catalytic subunit), and GAPDH were purchased from Abcam and were diluted to the suggested concentrations for Western blotting.

Subcellular Fractionation—HepG2 cells were harvested, and pellets were washed in $1\times$ PBS prior to resuspension in Dignam Buffer A (10 mM Tris, pH 7.6, 1.5 mM MgCl₂, 10 mM KCl, 0.5 mM DTT) and incubation on ice for 15 min. Cells were lysed by passage through a 25-gauge needle and centrifuged. The clear lysate was collected as the non-nuclear fraction (cytoplasm), and the pellet was resuspended in radioimmune precipitation assay buffer + propidium iodide and sonicated. Debris was pelleted by centrifugation and clear supernatant was collected as the nuclear fraction. 25 μ g of protein lysates was loaded onto 10% SDS-polyacrylamide gels and separated by electrophoresis. SREBP-2, PPP2CA, and GAPDH antibodies were used as described above, and anti-Lamin B (Santa Cruz Biotechnology, Inc.) was used as a nuclear marker. Anti-GAPDH (Rockland) was used as a cytosolic marker.

Immunocytochemistry Staining—48 h after HepG2 cells were transfected with control siRNA or PPP2CA siRNA, they were treated with 60 μ M lovastatin or DMSO for 6 h. They were then fixed and labeled with rabbit anti-LDLR antibody (Cayman Chemicals, Ann Arbor, MI), followed by incubation of Alexa Fluor 488-conjugated anti-rabbit secondary antibody (Invitrogen). After antibody incubation, cells were mounted with fluorescent mounting medium containing DAPI (Invitrogen) for counterstaining. Fluorescence microscopy was performed using a $20\times$ objective on a Leica DMI6000 confocal microscope, and images were processed using LAS AF software.

GFP-SREBP-2 Fluorescence Microscopy—HepG2 cells were transfected with control siRNA or PPP2CA siRNA, and 24 h later, EGFP-SREBP-2 was transfected into the cells by Lipofectamine 2000 (Invitrogen). The next day, the cells were treated with 40 μ M lovastatin or DMSO for 1 h. The cells were then fixed and mounted with DAPI-containing mounting buffer to visualize nuclei. The translocation of the SREBP-2 N terminus was examined by fluorescence microscopy (Leica DMI6000B).

LDL Uptake Assay—24 h after HepG2 cells were transfected with control siRNA or PPP2CA siRNA, they were washed with PBS and incubated overnight in lipoprotein-deficient medium to induce the expression of LDLR. The next day, cells were treated with 60 μ M lovastatin or DMSO for 6 h. LDL uptake was initiated by incubating cells grown in serum-deficient medium with 5 μ g/ml BODIPY-LDL (Invitrogen). Uptake of BODIPY-LDL was measured after a 30-min incubation at 37 °C. Cells were fixed and mounted with fluorescent mounting medium containing DAPI (Invitrogen) for counterstaining. Intercellular BODIPY-LDL was visualized using fluorescence microscopy.

Phosphatase Assays and Immunoprecipitation—Cells were trypsinized (Invitrogen) and immediately processed as follows. Cells were counted and resuspended in 1 ml of lysis buffer (50

mM Hepes, 0.1 mM EGTA, 0.1 mM EDTA, 120 mM NaCl, 0.5% Nonidet P-40, pH 7.5, 25 μ g/ml leupeptin, 25 μ g/ml pepstatin, 2 μ g/ml aprotinin, 1 mM PMSF) per 1×10^7 cells, as detailed in the DuoIC set PP2A phosphatase activity kit (R&D Systems).

In order to IP PP2A, protein was quantified with the Bradford Assay (Bio-Rad), and 1 mg of whole cell extract was precleared with 40 μ l of a 50% protein G-agarose slurry (Millipore) for 2 h at 4 °C. PP2A was immunoprecipitated overnight with 5 μ g of rat anti-PP2A (R&D Systems) at 4 °C. Immunocomplexes were collected with 20 μ l of protein G-agarose for 1 h at 4 °C. The protein G-agarose was washed two times with 1 ml of wash solution (0.05% Tween 20 in $1\times$ PBS, pH 7.2) at 4 °C for 5 min. Proteins were boiled off of the agarose in $2\times$ SDS-PAGE loading buffer at 100 °C for 10 min, and total IP lysate was loaded onto 10% polyacrylamide gels for Western analysis. Blots were probed for with anti-PPP2CA, anti-SREBP-2, and anti-GAPDH (Abcam). SREBP-2 was immunoprecipitated using 5 μ g of a SREBP-2 monoclonal antibody from Millipore. For nuclear co-immunoprecipitation, the nuclear IP kit from Active Motif was used according to the manufacturer's instructions.

Phosphorylation Analysis of SREBP-2—Cells were incubated in the absence or presence of lovastatin and either *Csi* or *PPP2CA_{si}*. Cell-free lysates were obtained, and total phosphothreonine-, phosphoserine-, or phosphotyrosine-phosphorylated proteins were immunoprecipitated using polyclonal antibodies against phosphothreonine, phosphoserine, or phosphotyrosine (1:1,000 dilutions) (Sigma). Immunoprecipitates were resolved by SDS-PAGE and transferred to nitrocellulose membranes. The degree of phosphorylated SREBP-2 present was determined by Western analysis, using anti-SREBP-2 polyclonal antibodies (1:250 dilution). For the corollary experiment, SREBP-2 was immunoprecipitated using anti-SREBP-2 antibodies, and the degree of phosphorylation was determined using anti-phosphoantibodies and Western analysis. Densitometry was performed using ImageQuant software.

Chromatin Immunoprecipitation Analysis of the DNA Binding Activity of SREBP-2—Cells grown in the absence or presence of statin were treated with 1% formaldehyde for 15 min at room temperature. Cross-linking was stopped by the addition of 125 mM glycine. Cells were washed, pelleted, and washed with PBS. Cells were then lysed using lysis buffer (50 mM HEPES, pH 7.5, containing 140 mM NaCl, 0.1% Triton X-100, 0.1% sodium deoxycholate, and a protease mixture) and spun down to remove cellular debris. 1 mg of the resulting supernatant was used for immunoprecipitating SREBP-2-bound DNA for 1 day at 4 °C, using 5 μ g of anti-SREBP-2 polyclonal antibodies.

Immunoprecipitated complexes were isolated after 1 h at 4 °C using protein A-agarose beads with salmon sperm DNA (Millipore). The beads were washed with lysis buffer containing 500 mM NaCl, and finally with 10 mM Tris-HCl, pH 8.0, containing 0.25 M LiCl, 0.5% Nonidet P-40, 0.5% sodium deoxycholate, followed by a wash with Tris-EDTA, pH 8.0. SREBP-2-DNA complexes were eluted from beads using 50 mM Tris-HCl, pH 8.0, containing 10 mM EDTA, and 1% SDS. Cross-linking was reversed using 5 M NaCl at 65 °C for 6 h. Samples were then diluted using 500 mM Tris-HCl, pH 8.0, containing 10 mM EDTA and 0.67% SDS. Samples were treated with 250 μ g

of Proteinase K for 1 h at 37 °C. DNA was eluted from samples using the DNA Easy kit (Qiagen). Purified DNA was used to PCR-amplify bound DNA. PCR products were resolved by 1.5% agarose gel electrophoresis.

Cyclohexamide Protein Stability Assay—HepG2 cells were grown in minimum Eagle's medium supplemented with 10% FBS, 1% sodium pyruvate, 1% L-glutamine, and 1% non-essential amino acids. All cells were plated on collagen-coated plates and incubated at 37 °C, 5% CO₂. 100 nM *Csi* or *PPP2Casi* (Dharmacon) was transfected at 48 and 24 h prior to statin treatment using dharmafect 4 transfection reagent. Cells were then treated with 75 μM lovastatin (Sigma) for 24 h. Cells were then treated with 5 μg/ml cyclohexamide for 0, 1, 2, 4, and 8 h. Cells were harvested, washed in 1× PBS (Sigma), and stored at -80 °C until processing.

Cells were resuspended in 1× radioimmune precipitation assay buffer and sonicated at 4 °C on ice for 10 min (30-s on, 30-s off cycle). Cell debris was pelleted by centrifugation for 10 min, and cell lysates were collected and analyzed for protein content using the Bradford assay. Whole cell extract was boiled at 100 °C for 10 min and loaded onto a 15% denaturing gel and run at 100 V for 90 min. Proteins were then transferred to nitrocellulose using the iBlot transfer device (Invitrogen). Blots were blocked in 5% milk-TBST prior to incubation with anti-SREBP-2 (Abcam) and secondary anti-mouse HRP. Antibodies were detected using an ECL detection kit from Millipore and a charge-coupled device camera (GE ImageQuant LAS 4000).

Electrophoretic Mobility Shift Assay—Nuclear extracts were prepared from HepG2 cells using the nuclear extract kit (Active Motif, Carlsbad, CA) as described by the manufacturer. Wild type (WT) and mutant probes were synthesized as single-stranded oligonucleotides with Biotin 3'-end labeling (Integrated DNA Technology). The sequences of the probes used were as follows: LDLR SRE, WT forward (5'-GGTGAAGACA-TTTGAAAATCACCCACTGCAAACCTCCTCCCCCTGC-TAGAA-3') and reverse (5'-TTCTAGCAGGGGGAGGAGT-TTGCAGTGGGGTGATTTTCAAATGTCTTCACC-3'); mutant forward (5'-GGTGAAGACATTTGAAAATGAGGG-GAGTGCAAACCTCCTTCTCTGCTAGAA-3') and reverse (5'-TTCTAGCAGGAAGAGGAGTTTGCCTCCCCTCAT-TTCAAATGTCTTCACC-3').

EMSA binding reactions were performed at room temperature for 30 min and consisted of nuclear extract in 1× binding buffer (50% glycerol, 100 mM MgCl₂, 1 μg/μl poly(dI-dC), 1% Nonidet P-40, 1 M KCl, 100 mM EDTA, and 5 μM DNA probe). The mixture was run on 6% non-denaturing polyacrylamide gels in 1× Tris borate-EDTA buffer. Protein-DNA complexes were then transferred to Hybond-N⁺ nylon membrane using the Trans-Blot semidry method (Bio-Rad) and cross-linked using the Spectrolinker XL-1000 UC cross-linker (Spectronics Corp.). Detection of biotin-labeled DNA was performed using the LightShift chemiluminescent EMSA kit (Thermo Scientific) and visualized by exposure to a charge-coupled device camera (GE ImageQuant LAS 4000).

For EMSA competition studies, a 10-fold molar excess of WT non-biotin-labeled forward and reverse oligonucleotides was added to the EMSA reaction mix. For the supershift assay, 6 μg of SREBP-2 mouse antibody (Abcam) was added to the reaction

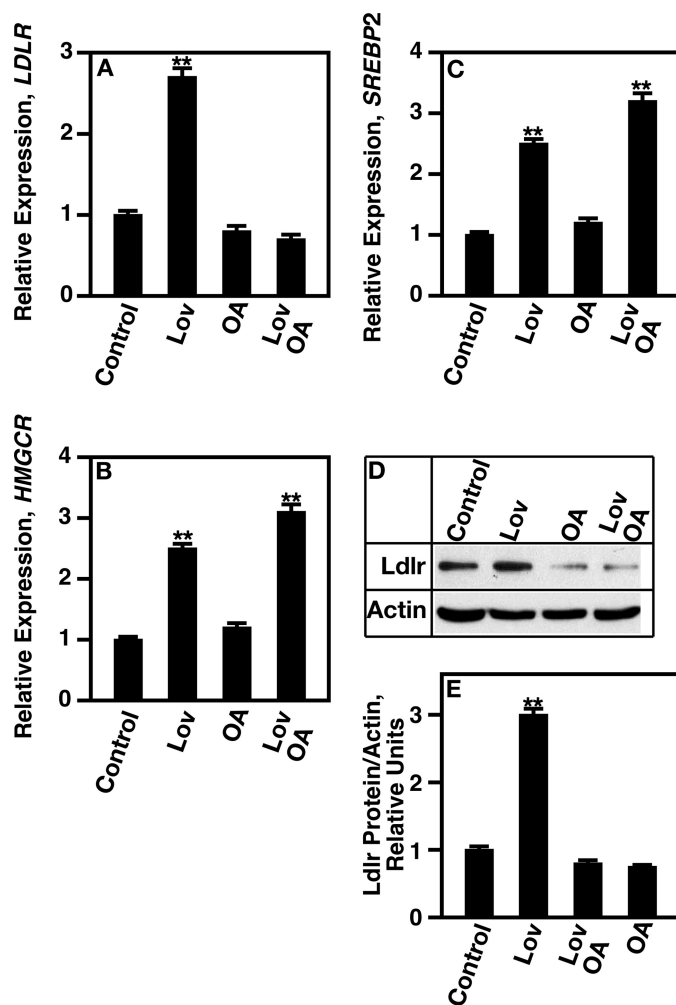


FIGURE 1. Okadaic acid inhibits lovastatin-induced gene expression. HepG2 cells were grown as described under "Experimental Procedures," in the absence or presence of lovastatin (*Lov*), okadaic acid (*OA*), or lovastatin and okadaic acid (*Lov OA*) for 24 h. The PP2A inhibitor okadaic acid (10 nM) was added for the final 8 h, mRNA expression was determined using qRT-PCR, and protein level was determined by Western analysis using polyclonal antibodies. *A*, relative level of *LDLR* expression. *B*, relative level of *SREBP-2* expression. *C*, relative level of *HMGCR* expression. *D*, *Ldlr* protein levels. *E*, relative densitometry units calculated using *Ldlr* protein levels in *D*. **, $p < 0.001$. Error bars, S.E.

mixture. The mixture was fractionated on a 6% non-denaturing polyacrylamide gel. Transfer and detection were performed as described above.

RESULTS

The Protein Phosphatase Inhibitor Okadaic Acid Blocks SREBP-2-dependent LDLR Gene Expression—To determine whether PP2A was required for *LDLR* gene expression, PP2A activity was chemically reduced using 10 nM OA, and SREBP-2 was indirectly activated using the HMGR inhibitor, lovastatin. The relative levels of *LDLR* gene expression and protein were determined. PP2A phosphatase activity was decreased by >85% at this OA concentration (data not shown). The level of cell cholesterol was decreased by 30% (data not shown).

OA treatment had little effect on basal *LDLR* expression as determined by qRT-PCR (Fig. 1*A*, *Control* versus *OA*). In the presence of lovastatin, *LDLR* gene expression increased by

Regulation of LDL-C Uptake by PP2A

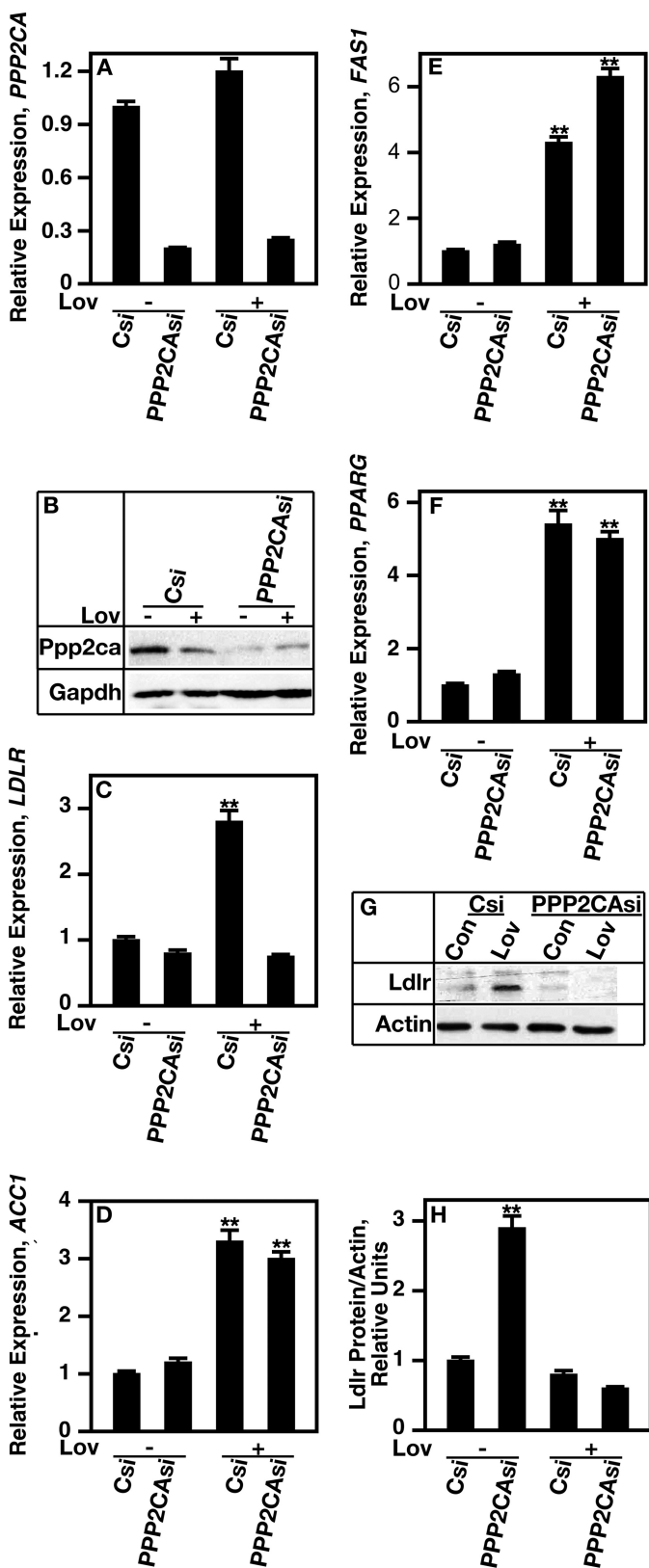


FIGURE 2. siRNA directed against PP2A inhibits lovastatin-induced gene expression. HepG2 cells were grown as described under "Experimental Procedures," in the absence (–Lov) or presence (+Lov) of lovastatin. Cells were treated with 100 nm non-targeting siRNA (Csi) or siRNA directed against the α catalytic subunit of PP2A (PPP2CA^{si}) at 48 and 24 h prior to lovastatin treatment. 75 μ M lovastatin was added for 24 h, and cells were harvested. mRNA expression was determined using qRT-PCR. *A*, relative expression of PPP2CA. *B*, protein level of Ppp2ca. *C*, relative level of LDLR expression. *D*, relative level of ACC1 expression. *E*, relative level of FAS1 expression. *F*, relative level of PPAR γ expression. *G*, Ldlr protein levels. *H*, relative densitometry units calculated using Ldlr protein levels in *G*. **, $p < 0.001$. GAPDH, glyceraldehyde phosphate dehydrogenase, loading control. Error bars, S.E.

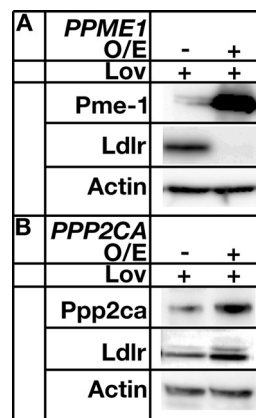


FIGURE 3. Altering the methylation status of Ppp2ca results in decreased SREBP-2 activity. HepG2 cells were transiently transfected with overexpression plasmids pCMV-PPME1 or pCMV-PPP2CA and were grown in the presence of 75 μ M lovastatin for 24 h. Cells were harvested, and protein levels were determined by Western analysis. *A*, protein levels of Pme-1 and Ldlr. *B*, protein levels of Ppp2ca and Ldlr. **, $p < 0.001$. Actin, loading control.

~2.5-fold (Fig. 1A, Control versus Lov). This -fold increase is in good agreement with previous data (32, 33). No increase in expression was seen in cells treated with lovastatin and OA (Fig. 1A, Lov versus Lov OA). OA treatment had no effect on lovastatin-induced expressions of HMGCR and SREBP-2 (Fig. 1, B and C). Ldlr protein level increased ~3.0-fold in response to lovastatin treatment, whereas there was no increase when PP2A activity was abolished (Fig. 1, B and C). Treatment with the cholesterol-depleting agent hydroxypropyl- β -cyclodextrin or simvastatin/atorvastatin gave similar results (not shown).

PP2A Is Required for SREBP-2-dependent Sterol Gene Expression—Because OA (>10 nM) can inhibit other protein phosphatases, PP2A activity was reduced using siRNA methods. siRNA against the α catalytic subunit of PP2A was used to reduce activity (PPP2CA^{si}).

PPP2CA^{si} treatment decreased PPP2CA gene expression and protein by >90% (Fig. 2, A and B, Csi versus PPP2CA^{si}). Control cells had a 2.5-fold increase in LDLR expression in response to lovastatin (Fig. 2C, Csi versus Csi Lov). Ppp2ca depletion abolished this increase (Fig. 2C, PPP2CA^{si} versus PPP2CA^{si} Lov). The depletion of Ppp2ca had no effect on the expressions of SREBP-1c-dependent genes, including acetyl coxylase (ACC1), fatty acid synthase (FAS1), and PPAR γ (PPARG) (Fig. 2, D–F, PPP2CA^{si} versus PPP2CA^{si} Lov). Ldlr protein increased 2.0-fold in control cells in response to lovastatin (Fig. 2, G and H, Csi, Con versus Lov) but not in Ppp2ca-depleted cells (Fig. 2, G and H, PPP2CA^{si}, Con versus Lov). Similar results were obtained using THLE-3 cells and rat primary hepatocytes (not shown).

Overexpression of the Protein Phosphatase 2A Methyltransferase Results in the Loss of PP2A-dependent LDLR Gene Expression—The catalytic subunit of PP2A is demethylated on Lys-309 by the Pme-1 demethylase (PPME1), causing a reduction in phosphatase activity (34).

B, protein level of Ppp2ca. *C*, relative level of LDLR expression. *D*, relative level of ACC1 expression. *E*, relative level of FAS1 expression. *F*, relative level of PPAR γ expression. *G*, Ldlr protein levels. *H*, relative densitometry units calculated using Ldlr protein levels in *G*. **, $p < 0.001$. GAPDH, glyceraldehyde phosphate dehydrogenase, loading control. Error bars, S.E.

To further substantiate the requirement of PP2A for *LDLR* expression, *PPME1* or the *PPP2CA* catalytic subunit of PP2A was overexpressed, and *LDLR* expression and protein were determined. Ectopic overexpression of *PPME1* resulted in ~7-fold overexpression of protein (Fig. 3A), whereas Ppp2ca was overexpressed by ~5-fold (Fig. 3B).

The overexpression of *PPME1* decreased lovastatin-induced *LDLR* expression by ~75%, whereas *PPP2CA* overexpression caused an additional 4-fold increase over drug-treated control cells (not shown). *Ldlr* protein level was decreased in Pme-1-

overexpressing cells (Fig. 3A), whereas it was increased when Ppp2ca was overexpressed (Fig. 3B).

PP2A Is Not Required for Lovastatin-induced SREBP-2 Processing and Nuclear Translocation—When the level of cholesterol is high, full-length SREBP-2 localizes to the endoplasmic reticulum as an inactive protein. When the level of cholesterol becomes decreased, it traffics to the Golgi (20, 35), where it is proteolytically cleaved, releasing a soluble active transcription factor (SREBP-2af) that translocates to the nucleus, where it induces cholesterol gene expression by binding to SREs.

To begin to determine the step where PP2A regulates SREBP-2 activity, SREBP-2 proteolytic processing and nuclear translocation were examined in Ppp2ca-depleted cells. A nuclear fraction was used for these experiments and was purified by subcellular fractionation and ultracentrifugation. Fraction purity was assessed by Western analysis using antibodies directed against nuclear Lamin B and cytosolic Gapdh (Fig. 4).

SREBP-2af accumulated in the nucleus in response to lovastatin treatment (Fig. 4, *Csi, Con versus Lov*). Similar results were seen when Ppp2ca was depleted (Fig. 4, *Csi Lov versus PPP2CAsi Lov*). A higher basal level of SREBP-2af was observed in the nucleus in the absence of Ppp2ca and lovastatin (Fig. 4, *PPP2CAsi versus Csi*). Based on this result, we cannot definitively rule out the possibility that PP2A does not have a negative role in proteolytic processing. However, there was an additional increase in *SREBP-2af* nuclear localization in the presence of lovastatin and absence of Ppp2ca. Moreover, *LDLR* gene expression was not increased in the absence of lovastatin in Ppp2ca-depleted cells (Fig. 2).

To further show that SREBP-2af translocates to the nucleus in the absence of Ppp2ca, the localization of a N-terminal full-length GFP-SREBP-2 was visualized by fluorescence microscopy, in the absence and presence of Ppp2ca and lovastatin. SREBP-2 nuclear translocation and function was also assessed indirectly by determining the degree of LDL-C uptake using fluorescence microscopy.

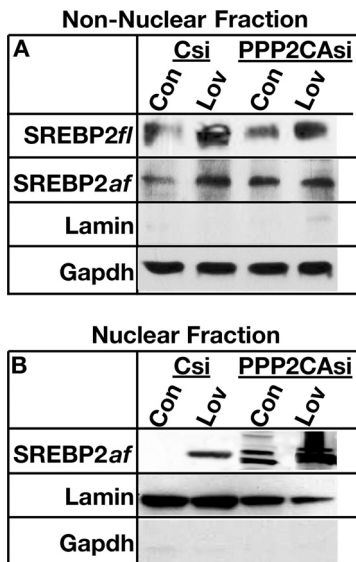


FIGURE 4. Loss of Ppp2ca does not affect SREBP-2 cleavage and nuclear translocation. HepG2 cells were grown in the absence (Con) or presence of lovastatin (Lov). Cells were treated with 100 nM non-targeting siRNA (Csi) or siRNA directed against the catalytic subunit of PP2A (PPP2CAsi) at 48 and 24 h prior to lovastatin treatment. 75 μ M lovastatin was added for 24 h, and cells were harvested. Cells were lysed and centrifuged as described under "Experimental Procedures" in order to obtain nuclear fractions. Cell protein was resolved by SDS-PAGE, and proteins were detected using Western analysis. Lamin was used as a nuclear marker. Gapdh was used as a non-nuclear marker. SREBP-2af, cleaved SREBP-2. A, non-nuclear fraction. B, nuclear fraction.

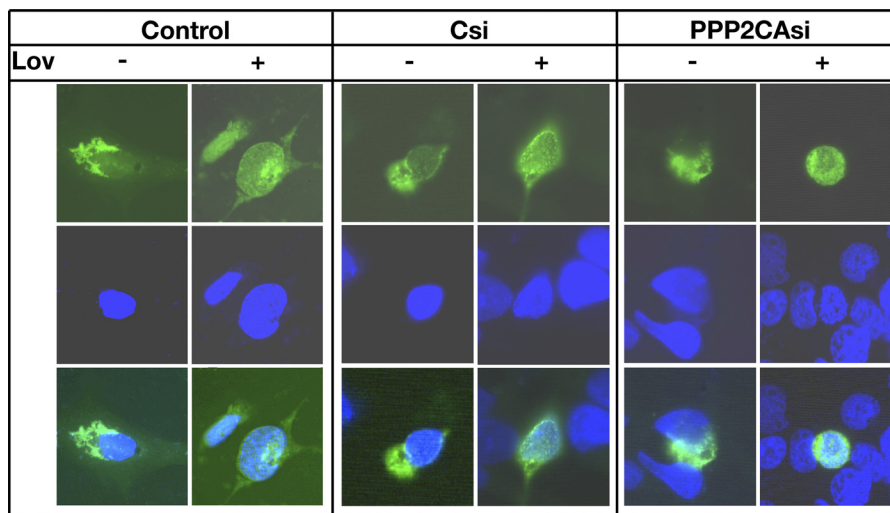


FIGURE 5. GFP-SREBP-2 translocates into the nucleus in cells lacking PP2A. HepG2 cells were transfected with no siRNA (Control), control siRNA (Csi), or siRNA directed against the catalytic subunit of PP2A (PPP2CAsi), in the absence (-Lov) or presence (+Lov) of lovastatin. pEGFP-SREBP-2 was transfected into cells that were subsequently treated with 40 μ M lovastatin or DMSO for 1 h, fixed, and mounted with DAPI-containing mounting buffer to visualize nuclei. The movement of GFP-SREBP-2 was examined by fluorescence microscopy (Leica DMI6000B).

Regulation of LDL-C Uptake by PP2A

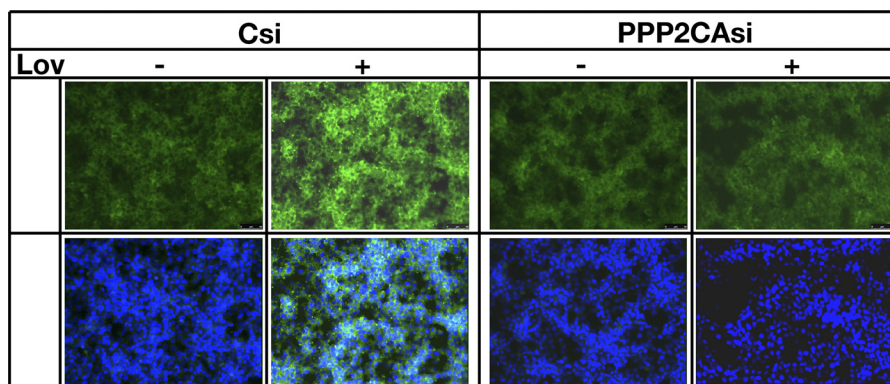


FIGURE 6. LDL-C uptake is defective in cells lacking Ppp2ca. HepG2 cells were transfected with control siRNA (*Csi*) or siRNA directed against the catalytic subunit of PP2A (*PPP2Casi*) and were incubated for 16 h in lipoprotein-deficient medium to induce the expression of Ldlr. Cells were treated with 60 μ M lovastatin or DMSO for 6 h. LDL-C uptake was initiated by incubating cells with 5 μ g/ml BODIPY-LDL. Uptake of BODIPY-LDL was measured after 30 min at 37 °C. Cells were fixed and mounted with fluorescent mounting medium containing DAPI for counterstaining. Intercellular BODIPY-LDL was visualized using fluorescence microscopy.

In untreated control cells, GFP-SREBP-2 localized to a perinuclear organelle (Fig. 5, *control*) that co-stained with the ER marker, PDI (*not shown*). Upon the addition of lovastatin, full-length GFP-SREBP-2 was cleaved, and GFP-SREBP $_{af}$ translocated to the nucleus (Fig. 5, *Control + Lov*). Similar results were obtained using cells transfected with a control siRNA (Fig. 5, *Csi versus Csi + Lov*). The loss of the Ppp2ca had no effect on SREBP-2 $_{af}$ translocation in the presence of lovastatin (Fig. 5, *PPP2Casi versus PPP2Casi + Lov*). Greater than 90% of transfected cells had the localization patterns shown.

LDL-C Uptake Requires PP2A—LDL-C uptake was assayed using the fluorescence-labeled lipid, BODIPY-LDL. In the absence of lovastatin, control cells had little BODIPY-LDL staining (Fig. 6, *Csi - Lov*). Upon the addition of lovastatin, a drastic increase was seen in intercellular BODIPY-LDL staining, indicative of increased LDL-C uptake (Fig. 6, *Csi + Lov*). Loss of Ppp2ca resulted in loss of BODIPY-LDL uptake in the presence of lovastatin (Fig. 6, *PPP2Casi - Lov versus PPP2Casi + Lov*).

PP2A Is Required for SREBP-2 DNA Binding to a LDLR SRE in Response to Lovastatin Treatment—The fact that SREBP-2 $_{af}$ translocated to the nucleus in the absence of Ppp2ca indicated that its function was regulated at a point downstream of transport and nuclear entry, quite possibly at the point of promoter binding. Thus, SREBP-2 $_{af}$ SRE promoter binding was assayed in the absence and presence of Ppp2ca and lovastatin using ChIP and EMSA.

ChIP analyses revealed that under basal conditions, Ppp2ca depletion slightly altered SREBP-2 $_{af}$ binding to a *LDLR* promoter SRE in the absence of lovastatin, when compared with untreated cells (Fig. 7, *A and B, Csi - Lov versus PPP2Casi - Lov*). Whereas a 5-fold increase in binding was seen in the presence of both lovastatin and Ppp2ca (Fig. 7, *A and B, Csi - Lov versus Csi + Lov*), Ppp2ca-depleted cells showed a decrease in SREBP-2 $_{af}$ *LDLR* promoter binding in the presence of lovastatin (Fig. 7, *A and B, Csi + Lov versus PPP2Casi + Lov*). Ppp2ca depletion had no effect on lovastatin-induced binding to a *HMGCR* SRE (Fig. 7, *A and B, Csi + Lov versus PPP2Casi + Lov*).

EMSA analysis was next performed using wild type and mutant *LDLR* SREs. Under cholesterol-rich conditions in the

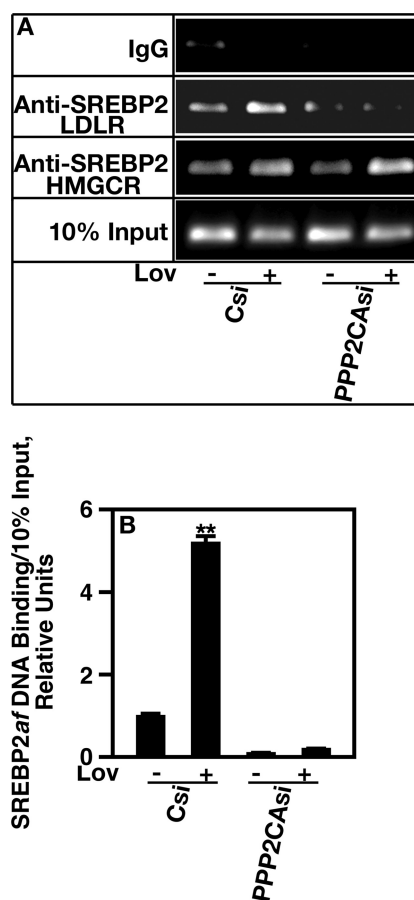


FIGURE 7. Loss of Ppp2ca causes a reduction in SREBP-2 LDLR SRE binding. Cells transfected with control siRNA (*Csi*) or siRNA directed against the catalytic subunit of PP2A (*PPP2Casi*) were grown for 6 h in the absence ($-$ Lov) or presence ($+$ Lov) of lovastatin. Cells were then treated with 1% formaldehyde to cross-link SREBP-2 to DNA. The cross-linking reaction was terminated, and SREBP-2-DNA complexes were isolated using anti-SREBP-2 polyclonal antibodies. SREBP-2-DNA cross-links were disrupted using 5 M NaCl. *A*, amount of SREBP-2-bound DNA determined by PCR amplification and agarose gel electrophoresis. *B*, relative densitometry unit ratio of SREBP-2 SRE binding versus IgG binding. 10% of input, loading control; IgG, negative control. Error bars, S.E.

presence of Ppp2ca, SREBP-2 $_{af}$ displayed a low basal level of binding to the WT SRE (Fig. 8*A, Con Ppp2ca, lane 3*). Binding was seen as a doublet. The binding was specific because no

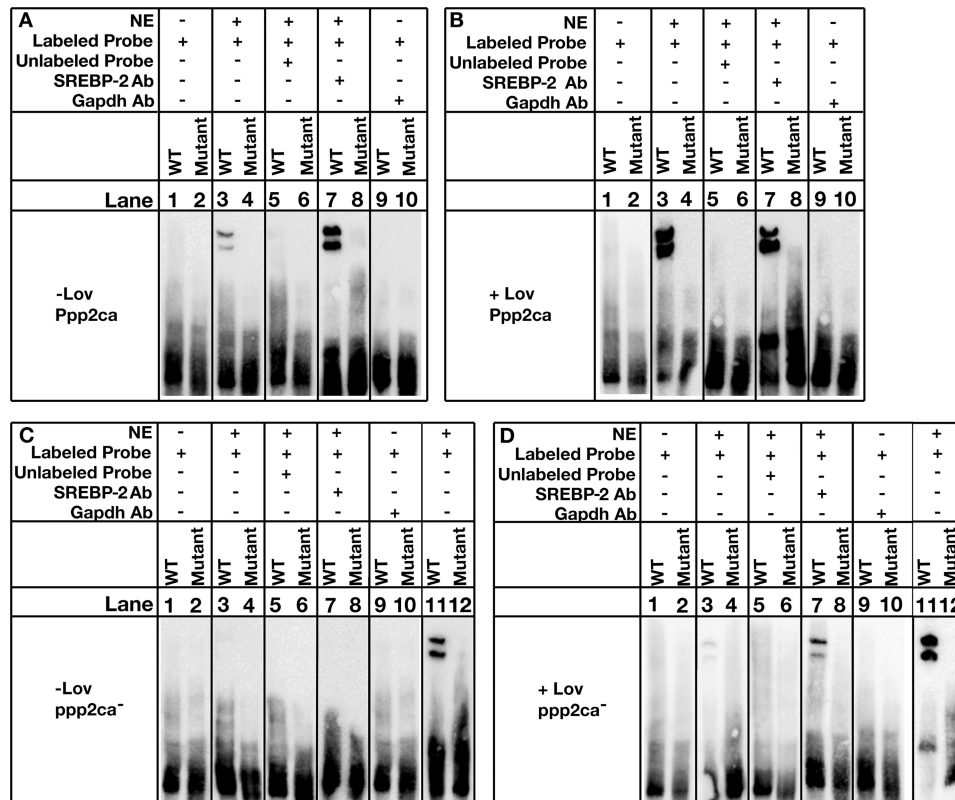


FIGURE 8. Ppp2ca is required for direct binding of SREBP-2 to a LDLR SRE. Nuclear extracts were prepared from HepG2 cells using a nuclear extract kit. WT and mutant probes were synthesized as single-stranded oligonucleotides. The sequences are given under "Experimental Procedures." Nuclear extracts (NE) containing a biotinylated probe (*Labeled Probe*) were resolved on 6% non-denaturing polyacrylamide gels. Protein-DNA complexes were then transferred to Hybond-N⁺ nylon membranes and cross-linked. Detection of biotin-labeled DNA was performed using chemiluminescence and visualized by exposure to a charge-coupled device camera. For competition studies, a 10-fold molar excess of WT non-biotin labeled oligonucleotides (*Unlabeled Probe*) was used. For supershift experiments, SREBP-2 antibodies were added to the reaction mixture (*SREBP-2 Ab*). Gapdh antibodies were used as a negative control (*Gapdh Ab*). *A*, nuclear extracts were obtained from cells containing Ppp2ca in the absence of lovastatin (*-Lov Ppp2ca*). *B*, nuclear extracts were obtained from cells containing Ppp2ca in the presence of lovastatin (*Lov Ppp2ca*). *C*, nuclear extracts were obtained from cells lacking Ppp2ca in the absence of lovastatin (*-Lov ppp2ca⁻*). *D*, nuclear extracts were obtained from cells lacking Ppp2ca in the presence of lovastatin (*Lov ppp2ca⁻*).

binding was seen to a mutated SRE (*mutant*) (Fig. 8*A*, *Con Ppp2ca*, lane 4). The addition of excess unlabeled probe eliminated binding to the wild type SRE (Fig. 8*A*, *Con Ppp2ca*, lane 5). The addition of anti-SREBP-2 antibodies to the reaction caused an increase in band intensity (Fig. 8*A*, *Con Ppp2ca*, lane 7). This type of result, where the addition of antibody does not result in a supershift, still indicates specific binding and has been previously observed (36, 37). Binding was specific because no binding was observed to a mutated SRE in the presence of antibody (Fig. 8*A*, *Con Ppp2ca*, lane 8). Finally, the addition of anti-GAPDH antibodies to the labeled probe did not result in the appearance of bands (Fig. 8*A*, *Con Ppp2ca*, lane 9).

In the presence of lovastatin and Ppp2ca, WT promoter binding band intensity was increased, compared with that seen under cholesterol-rich conditions (Fig. 8*B*, *Lov Ppp2ca*, lane 3 versus Fig. 8*A*, *Con Ppp2ca*, lane 3). Promoter binding was specific (Fig. 8*B*, *Lov Ppp2ca*, lane 5), and the addition of GAPDH antibodies did not cause the appearance of nonspecific bands (Fig. 8*B*, *Lov Ppp2ca*, lane 9). When Ppp2ca was depleted, promoter binding was eliminated under cholesterol-rich conditions (Fig. 8*C*, *Con ppp2ca⁻*, lanes 3 and 7) and severely reduced in the presence of lovastatin (Fig. 8*D*, *Lov ppp2ca⁻*, lanes 3 and 7).

Loss of PP2A Does Not Alter the Half-life of SREBP-2—One possibility to explain the loss of SRE binding is that SREBP-2 is

degraded much faster in the absence of Ppp2ca. To address this question, the half-lives of nuclear SREBP-2 were determined in the presence and absence of lovastatin and Ppp2ca. In the absence of lovastatin and presence of Ppp2ca, SREBP-2af was degraded over a period of 8 h, with a half-life of ~4 h (Fig. 9, *A* and *B*, *Con*, *-Lov*). In contrast, SREBP-2 accumulated in the presence of both lovastatin and Ppp2ca (Fig. 9, *A* and *B*, *Con*, *+Lov*). Similar results were observed in the absence of Ppp2ca (Fig. 9, *A* and *C*, *PPP2si*, \pm *Lov*). Thus, the loss of SRE binding seen in the ChIP and EMSA studies was not due to increased degradation of SREBP-2 protein.

PP2A Binds SREBP-2—Co-immunoprecipitation was next used to determine whether Ppp2ca directly bound to SREBP-2af. Ppp2ca was immunoprecipitated, interacting proteins were resolved by SDS-PAGE, and Western analysis was used to detect SREBP-2af association. 10% inputs used in the co-immunoprecipitation experiments are shown in Fig. 9, *A* and *D*.

SREBP-2af was efficiently pulled down by Ppp2ca antibodies (Fig. 10*B*) but not the IgG antibody control. The Ppp2ca-SREBP-2af interaction was detected at all time points and in control and lovastatin-treated samples (not shown). Identical results were obtained when SREBP-2 antibodies were used to pull down Ppp2ca (Fig. 10*C*). SREBP-2af was also able to pull down the A subunit of PP2A, Ppp2r1a (not shown).

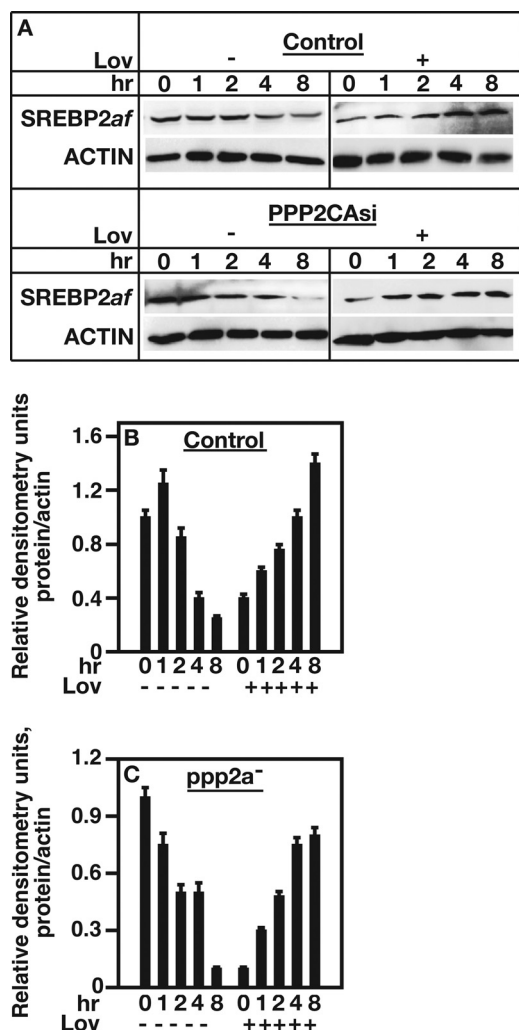


FIGURE 9. Loss of Ppp2ca has no effect on SREBP-2 half-life. HepG2 cells were transfected with 100 nM control siRNA (Con) or siRNA directed against the catalytic subunit of PP2A (PPP2CAsi) at -48 and -24 h in the absence ($-Lov$) and presence ($+Lov$) of lovastatin treatment. Cells were treated with $75 \mu\text{M}$ lovastatin for 24 h. Cells were treated with $5 \mu\text{g/ml}$ cyclohexamide for the indicated times, harvested, and stored at -80°C until processing. Whole cell extracts were resolved using a 15% denaturing SDS-PAGE gel. Proteins were transferred to nitrocellulose and incubated with SREBP-2 antibodies. Protein was detected using ECL chemiluminescence. *Actin*, loading control. *Error bars*, S.E. *A*, Western analysis of SREBP-2 protein. *B*, densitometry of protein in control cells. *C*, densitometry of protein in ppp2a cells.

If Ppp2ca directly regulates nuclear SREBP-2af DNA binding, then it should associate with SREBP-2af in the nucleus. Nuclear SREBP-2af was efficiently co-immunoprecipitated in the absence or presence of lovastatin using Ppp2ca antibodies (Fig. 10E). SREBP-2 antibodies were able to pull down nuclear Ppp2ca (Fig. 10F).

Loss of PP2A Alters the Phosphorylation State of SREBP-2af—The direct interaction between Ppp2ca and SREBP-2af suggests that PP2A may modulate SREBP-2af phosphorylation status, causing changes in DNA binding. If this is the case, then the phosphorylation status of SREBP-2af should be altered in cells lacking Ppp2ca. Phosphorylated proteins were immunoprecipitated using phosphospecific antibodies, and SREBP-2af phosphorylation was determined by Western analysis using anti-SREBP-2 antibodies.

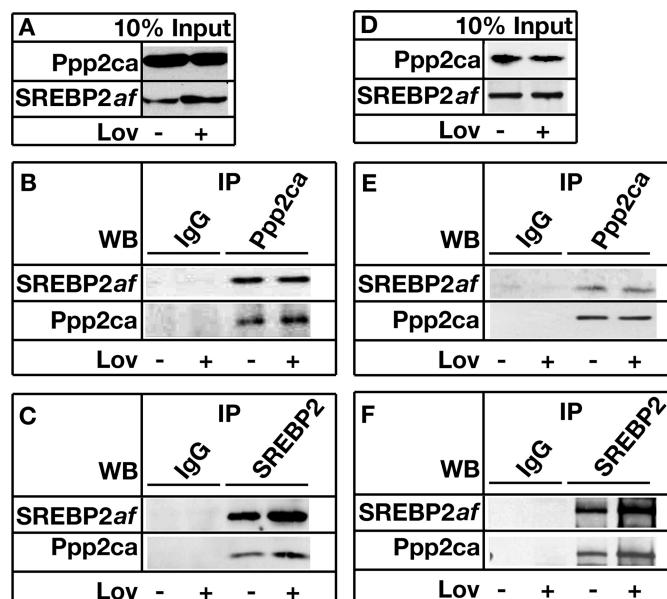


FIGURE 10. Ppp2ca interacts with SREBP-2. HepG2 cells were grown in the absence ($-Lov$) or presence ($+Lov$) of lovastatin. $75 \mu\text{M}$ lovastatin was added for 24 h. Whole cell lysates were obtained by sonication and centrifugation. Nuclear extracts were obtained as described under "Experimental Procedures." Ppp2ca was immunoprecipitated (IP) using rat anti-Ppp2ca polyclonal antibodies. SREBP-2 was immunoprecipitated using SREBP-2 antibodies. Immunoprecipitated proteins were resolved by SDS-PAGE, and proteins were detected using Western analysis (WB). *A*, 10% of the whole cell extract used. *B*, immunoprecipitation of SREBP-2 using anti-Ppp2ca antibodies. *C*, immunoprecipitation of Ppp2ca using SREBP-2 antibodies. *D*, 10% of the nuclear extract used. *E*, immunoprecipitation of SREBP-2 using anti-Ppp2ca antibodies. *F*, immunoprecipitation of Ppp2ca using SREBP-2 antibodies. *IgG*, negative control.

For all experiments, 1) an equal level of SREBP-2af was used, 2) PPP2CAsi knockdown efficiency was $>90\%$, 3) IgG immunoprecipitation experiments were used to demonstrate specificity, and 4) the specificity of each phosphoantibody was validated using phosphospecific blockers.⁴

In the absence of lovastatin, cells had a basal level of serine phosphorylation in the absence of lovastatin, which decreased 10-fold upon the addition of drug (Fig. 10A, *Csi versus Csi + Lov*). Threonine phosphorylation was absent in untreated cells but increased 3-fold in lovastatin-treated cells (Fig. 10B, *Csi versus Csi + Lov*).

In cells lacking Ppp2ca, the basal levels of SREBP-2af serine and threonine phosphorylation were increased in the absence of lovastatin (Fig. 11, *A and B, PPP2CAsi -Lov*), whereas both serine (12-fold) and threonine (7-fold) phosphorylation increased in Ppp2ca-depleted drug-treated cells (Fig. 11, *A and B, PPP2CAsi, -Lov versus PPP2CAsi +Lov*). No tyrosine phosphorylation was seen under all conditions (Fig. 11C). Similar results were obtained when SREBP-2 antibodies were used and Western analysis was performed using phosphospecific antibodies (not shown). Thus, the loss of Ppp2ca activity resulted in changes in the phosphorylation status of SREBP-2af that correlate with a loss of DNA binding and reduced LDL uptake.

DISCUSSION

The data show that PP2A regulates SREBP-2 activity and LDL-C uptake. Depletion of Ppp2ca resulted in the loss of

⁴ M. Villamil and J. T. Nickels, unpublished data.

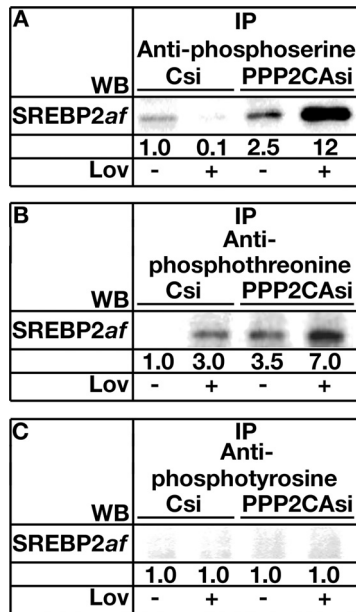


FIGURE 11. Loss of Ppp2ca changes the phosphorylation state of SREBP-2. HepG2 cells were grown in the absence ($-Lov$) or presence ($+Lov$) of lovastatin. Cells were treated with 100 nM non-targeting siRNA (*Csi*) or siRNA directed against the catalytic subunit of PP2A (*PPP2CAsi*) at 48 and 24 h prior to lovastatin treatment. 75 μ M lovastatin was added for 24 h. Cells were sonicated, cellular debris was pelleted by centrifugation, and cell lysates were collected. *A*, *B*, and *C*, phosphothreonine, phosphoserine, or phosphotyrosine proteins were used, immunoprecipitated (*IP*) by anti-phosphospecific polyclonal antibodies. Phosphorylated proteins were resolved by SDS-PAGE. The level of SREBP-2 phosphorylation was determined by Western analysis (*WB*) using SREBP-2 antibodies. The numbers represent relative densitometry units. All values are compared with their respective basal *Csi* value.

SREBP-2-dependent gene expression and SREBP-2af binding to an *LDLR* SRE promoter element. Ppp2ca regulation was specific to *LDLR* because the expressions of several other SREBP-2af genes were not affected. Loss of SREBP-2af binding was not due to increased degradation because the half-life of SREBP-2af was equivalent in the absence or presence of Ppp2ca. Ppp2ca regulated SREBP-2af SRE binding through a direct interaction that caused the dephosphorylation of several phosphoresidues required for function. Based on these data, we conclude that PP2A directly regulates SREBP-2af by regulating the phosphorylation status of serine/threonine residues required for DNA binding, *LDLR* gene expression, and LDL-C uptake.

Several phosphorylation events regulate SREBP function, where activity is stimulated or inhibited depending on the targeting kinase (38–47). For instance, ERK1/2-dependent SREBP-2 phosphorylation of Ser-455 increases its activity by blocking a sumoylation event inhibiting binding to the co-repressor, HDAC3. Glycogen synthase kinase-3 β phosphorylation of SREBP-1a on Thr-426 and Ser-430 initiates its degradation when bound to promoter regions of sterol-responsive genes, through targeting it for ubiquitin-dependent SCF-mediated degradation. AMP-activated protein kinase kinase inhibits SREBP-1c activity by phosphorylating Ser-372 within the soluble active fragment (48). Ser-117 on SREBP-1a is a major phosphorylation site for MAPK signaling (41). Thus, multiple phosphorylation events fine tune the activity of SREBPs. Which of these sites represent PP2A substrates needs to be elucidated to fully understand the depth of SREBP-2 regulation.

It is interesting that PP2A may only regulate SREBP-2. Differential specificities in the promoters of many sterol-responsive genes exist, including the *LDLR*, *HMGCR*, and *HMGCS* promoters (49). All display heterogeneity in their response to SREBP-1/SREBP-2 activity, by varying the number or sequence of various SREs or specific co-factor binding sites (50–54). The *LDLR* promoter responds to various signals based on the presence of multiple binding elements (55, 56), which includes the serum response, Sp1, repeat 3, Egr1, and *C/EBP β* elements (56, 57). Thus, PP2A may have a specific role in regulating cholesterol homeostasis through specific regulation of *LDLR* expression and LDL-C uptake.

PP2A regulates several metabolic processes. For example, it targets the basic helix-loop-helix leucine zipper carbohydrate-binding element-binding protein transcription factor (ChREBP). ChREBP target genes include those activating glycolysis, lipogenesis, and gluconeogenesis pathways (58), which contribute to the onset of metabolic syndrome (59). Although PP2A does activate ChREBP, possibly increasing the severity of metabolic syndrome, it has also been demonstrated that loss of PP2A through FoxO transcription factor inhibition may contribute to the onset of metabolic syndrome (60). These results indicate that PP2A activity is fine tuned in response to changes in global metabolism because those individuals with metabolic syndrome present with multiple maladies, including glucose intolerance or full-blown diabetes, high blood cholesterol level, obesity, and hypertension.

The PP2A AC dimer may always be bound to SREBP-2. Differential regulation may arise from the binding and release of different B subunits. It is unlikely that a single heterotrimeric species regulates nuclear transport, DNA binding, and transactivation. We have observed several B subunits accumulating in response to cholesterol depletion.⁵ It also makes sense that the expression of various B subunits be regulated through changes in cholesterol level. If multiple PP2A subpopulations are generated, depending on metabolic state, they can be turned on or off, depending on cholesterol level. A recent report showed that multiple PP2A subunits were regulated at the transcriptional, translational, and post-translational levels in myocytes (61).

Another possibility to explain phosphatase specificity is based on an emerging model suggesting that PP2A B subunits can act as “scaffolds” that enable AC dimer binding to a substrate under specific physiological conditions (62, 63). The B subunit is associated with a substrate alone and recruits the AC dimer at the appropriate time. The B56 β subunit complexes with Akt in the absence of the AC dimer and then recruits it to AKT upon insulin signaling (63). In the yeast *Saccharomyces cerevisiae*, the PP2A B subunit, ScCdc55, possesses an activity that may be separate from its association with a PP2A holoenzyme (64–66). We have recently found that a single B subunit is associated with SREBP-2 in mouse liver independent of the AC dimer.⁶ The “scaffold” model is still highly speculative and awaits further validation.

Finally, PP2A binding altered the phosphorylation status of SREBP-2af. Although most phosphorylation events regulating

⁵ L. Rice and J. T. Nickels, unpublished data.

⁶ B. Joseph, D. Pandya, and J. Nickels, manuscript in preparation.

SREBP activity cause increased protein degradation or induce the transactivation activity of promoter-bound protein, some exceptions exist. Very recently, AMP kinase was found to phosphorylate nuclear SREBP-2af, causing a decrease in SREBP-2-dependent gene expression (48). Moreover, it was shown that PKA phosphorylation of SREBP-1a/SREBP-1c reduces DNA binding (42). Whether these sites are PP2A targets remains to be elucidated.

Acknowledgments—We thank Drs. Martin Adelson, Eli Mordechai, and Siu Lo and Christina Segro for discussions. We also thank Suhani Chintan Pandya and Sophia Wurst for patience during the completion of the work.

REFERENCES

- Maxfield, F. R., and Tabas, I. (2005) Role of cholesterol and lipid and organization in disease. *Nature* **438**, 612–621
- Sonnino, S., and Prinetti, A. (2013) Membrane domains and the “lipid raft” concept. *Curr. Med. Chem.* **20**, 4–21
- Wood, W. G., Igbavboa, U., Müller, W. E., and Eckert, G. P. (2011) Cholesterol asymmetry in synaptic plasma membranes. *J. Neurochem.* **116**, 684–689
- Elson, E. L., Fried, E., Dolbow, J. E., and Genin, G. M. (2010) Phase separation in biological membranes. Integration of theory and experiment. *Annu. Rev. Biophys.* **39**, 207–226
- Incardona, J. P., and Eaton, S. (2000) Cholesterol in Signal Transduction. *Curr. Opin. Cell Biol.* **12**, 193–203
- Sato, K. (2008) Signal transduction of fertilization in frog eggs and anti-apoptotic mechanism in human cancer cells: common and specific functions of membrane microdomains. *Open Biochem. J.* **2**, 49–59
- Breitling, R. (2007) Greased hedgehogs: new links between hedgehog signaling and cholesterol metabolism. *Bioessays* **29**, 1085–1094
- Illingworth, D. R. (2000) Management of hypercholesterolemia. *Med. Clin. North Am.* **84**, 23–42
- Stein O, Stein, Y. (2005) Lipid transfer proteins (LTP) and atherosclerosis. *Atherosclerosis* **178**, 217–230
- Ni Chróinin, D., Asplund, K., Åsberg, S., Callaly, E., Cuadrado-Godia, E., Díez-Tejedor, E., Di Napoli, M., Engelter, S. T., Furie, K. L., Giannopoulos, S., Gotto, A. M., Jr., Hannon, N., Jonsson, F., Kapral, M. K., Martí-Fàbregas, J., Martínez-Sánchez, P., Milionis, H. J., Montaner, J., Muscari, A., Pikijs, S., Probstfield, J., Rost, N. S., Thrift, A. G., Vemmos, K., and Kelly, P. J. (2013) Statin therapy and outcome after ischemic stroke: systematic review and meta-analysis of observational studies and randomized trials. *Stroke* **44**, 448–456
- Ahmed M. H., and Byrne, C. D. (2008) Current treatment of non-alcoholic fatty liver disease. *Diabetes Obes. Metab.* **11**, 188–195
- Katz, S. (2008) Potential role of statins in the treatment of heart failure. *Curr. Atheroscler. Rep.* **10**, 318–323
- Palmer, S. C., Craig, J. C., Navaneethan, S. D., Tonelli, M., Pellegrini, F., and Strippoli, G. F. (2012) Benefits and harms of statin therapy for persons with chronic kidney disease: a systematic review and meta-analysis. *Ann. Intern. Med.* **157**, 263–275
- Upadhyay, A., Earley, A., Lamont, J. L., Haynes, S., Wanner, C., and Balk, E. M. (2012) Lipid-lowering therapy in persons with chronic kidney disease: a systematic review and meta-analysis. *Ann. Intern. Med.* **157**, 251–262
- Jukema, J. W., Cannon, C. P., de Craen, A. J., Westendorp, R. G., and Trompet, S. (2012) The controversies of statin therapy: weighing the evidence. *J. Am. Coll. Cardiol.* **60**, 875–881
- Tenenbaum, A., and Fisman, E. Z. (2012) Fibrates are an essential part of modern anti-dyslipidemic arsenal: spotlight on atherogenic dyslipidemia and residual risk reduction. *Cardiovasc. Diabetol.* **11**, 125
- Colbert, J. D., and Stone, J. A. (2012) Statin use and the risk of incident diabetes mellitus: a review of the literature. *Can. J. Cardiol.* **28**, 581–589
- Stein, E. A. (2013) Low-density lipoprotein cholesterol reduction by inhibition of PCSK9. *Curr. Opin. Lipidol.* **24**, 510–517
- Wang, X., Briggs, M. R., Hua, X., Yokoyama, C., Goldstein, J. L., and Brown, M. S. (1993) Nuclear protein that binds sterol regulatory element of low density lipoprotein receptor promoter. II. Purification and characterization. *J. Biol. Chem.* **268**, 14497–14504
- Sakai, J., Rawson, R. B., Espenshade, P. J., Cheng, D., Seegmiller, A. C., Goldstein, J. L., and Brown, M. S. (1998) Molecular identification of the sterol-regulated luminal protease that cleaves SREBPs and controls lipid composition of animal cells. *Mol. Cell* **2**, 505–514
- Brown, M. S., and Goldstein, J. L. (1997) The SREBP pathway: regulation of cholesterol metabolism by proteolysis of a membrane-bound transcription factor. *Cell* **89**, 331–340
- Cohen, P. T., Brewis, N. D., Hughes, V., and Mann, D. J. (1990) Protein serine/threonine phosphatases: an expanding family. *FEBS Lett.* **268**, 355–359
- Janssens, V., Longin, S., and Goris, J. (2008) PP2A holoenzyme assembly: in cauda venenum (the sting is in the tail) *Trends Biochem. Sci.* **33**, 113–121
- Hernández, M. L., Martínez, M. J., López de Heredia, M., and Ochoa, B. (1997) Protein phosphatase 1 and 2A inhibitors activate acyl-CoA:cholesterol acyltransferase and cholesterol ester formation in isolated rat hepatocytes. *Biochim. Biophys. Acta* **1349**, 233–241
- Jefcoate, C. R., Lee, J., Cherradi, N., Takemori, H., and Duan, H. (2011) cAMP stimulation of StAR expression and cholesterol metabolism is modulated by co-expression of labile suppressors of transcription and mRNA turnover. *Mol. Cell. Endocrinol.* **336**, 53–62
- Jones, P. M., Sayed, S. B., Persaud, S. J., Burns, C. J., Gyles, S., and Whitehouse, B. J. (2000) Cyclic AMP-induced expression of steroidogenic acute regulatory protein is dependent upon phosphoprotein phosphatase activities. *J. Mol. Endocrinol.* **24**, 233–239
- Wang, P. Y., Liu, P., Weng, J., Sontag, E., and Anderson, R. G. (2003) A cholesterol-regulated PP2A/HePTP complex with dual specificity ERK1/2 phosphatase activity. *EMBO J.* **22**, 2658–2667
- Wang, P. Y., Weng, J., and Anderson, R. G. (2005) OSBP is a cholesterol-regulated scaffolding protein in control of ERK 1/2 activation. *Science* **307**, 1472–1476
- Holen, I., Gordon, P. B., and Seglen, P. O. (1993) Inhibition of hepatocytic autophagy by okadaic acid and other protein phosphatase inhibitors. *Eur. J. Biochem.* **215**, 113–122
- Shen, L., Hillebrand, A., Wang, D. Q., and Liu, M. (2012) Isolation and primary culture of rat hepatic cells. *J. Vis. Exp.* 10.3791/3917
- Seglen, P. O. (1976) Preparation of isolated rat liver cells. *Methods Cell Biol.* **13**, 29–83
- Matsui, M., Sakurai, F., Elbashir, S., Foster, D. J., Manoharan, M., and Corey, D. R. (2010) Activation of LDL receptor expression by small RNAs complementary to a noncoding transcript that overlaps the LDLR promoter. *Chem. Biol.* **17**, 1344–1355
- Frey, T., and De Maio, A. (2007) Increased expression of CD14 in macrophages after inhibition of the cholesterol biosynthetic pathway by lovastatin. *Mol. Med.* **13**, 592–604
- Lee, J., and Stock, J. (1993) Protein phosphatase 2A catalytic subunit is methyl-esterified at its carboxyl terminus by a novel methyltransferase. *J. Biol. Chem.* **268**, 19192–19195
- Rawson, R. B., Zelenski, N. G., Nijhawan, D., Ye, J., Sakai, J., Hasan, M. T., Chang, T. Y., Brown, M. S., and Goldstein, J. L. (1997) Complementation cloning of S2P, a gene encoding a putative metalloprotease required for intramembrane cleavage of SREBPs. *Mol. Cell* **1**, 47–57
- Pallai, R., Bhaskar, A., Sodi, V., and Rice, L. M. (2012) Ets1 and Elk1 transcription factors regulate cancerous inhibitor of protein phosphatase 2A expression in cervical and endometrial carcinoma cells. *Transcription* **3**, 323–335
- Kurachi, S., Huo, J. S., Ameri, A., Zhang, K., Yoshizawa, A. C., and Kurachi, K. (2009) An age-related homeostasis mechanism is essential for spontaneous amelioration of hemophilia B Leyden. *Proc. Natl. Acad. Sci. U.S.A.* **106**, 7921–7926
- Sundqvist, A., Bengoechea-Alonso, M. T., Ye, X., Lukiyanchuk, V., Jin, J., Harper, J. W., and Ericsson, J. (2005) Control of lipid metabolism by phosphorylation-dependent degradation of the SREBP family of transcription

- factors by SCF(Fbw7). *Cell Metab.* **1**, 379–391
39. Kotzka, J., Lehr, S., Roth, G., Avci, H., Knebel, B., and Müller-Wieland, D. (2004) Insulin-activated Erk-mitogen-activated protein kinases phosphorylate sterol regulatory element-binding protein-2 at serine residues 432 and 455 *in vivo*. *J. Biol. Chem.* **279**, 22404–22411
 40. Wong, R. H., and Sul, H. S. (2010) Insulin signaling in fatty acid and fat synthesis: a transcriptional perspective. *Curr. Opin. Pharmacol.* **10**, 684–691
 41. Roth, G., Kotzka, J., Kremer, L., Lehr, S., Lohaus, C., Meyer, H. E., Krone, W., and Müller-Wieland, D. (2000) MAP kinases Erk1/2 phosphorylate sterol regulatory element-binding protein (SREBP)-1a at serine 117 *in vitro*. *J. Biol. Chem.* **275**, 33302–33307
 42. Lu, M., and Shyy, J. Y. (2006) Sterol regulatory element-binding protein 1 is negatively modulated by PKA phosphorylation. *Am. J. Physiol. Cell Physiol.* **290**, C1477–C1486
 43. Punga, T., Bengochea-Alonso, M. T., and Ericsson, J. (2006) Phosphorylation and ubiquitination of the transcription factor sterol regulatory element-binding protein-1 in response to DNA binding. *J. Biol. Chem.* **281**, 25278–25286
 44. Bengochea-Alonso, M. T., and Ericsson, J. (2006) Cdk1/cyclin B-mediated phosphorylation stabilizes SREBP1 during mitosis. *Cell Cycle* **5**, 1708–1718
 45. Kotzka, J., Knebel, B., Haas, J., Kremer, L., Jacob, S., Hartwig, S., Nitzgen, U., and Müller-Wieland, D. (2012) Preventing phosphorylation of sterol regulatory element-binding protein 1a by MAP-kinases protects mice from fatty liver and visceral obesity. *PLoS One* **7**, e32609
 46. Kotzka, J., Knebel, B., Avci, H., Jacob, S., Nitzgen, U., Jockenhovel, F., Heeren, J., Haas, J., and Müller-Wieland, D. (2010) Phosphorylation of sterol regulatory element-binding protein (SREBP)-1a links growth hormone action to lipid metabolism in hepatocytes. *Atherosclerosis* **213**, 156–165
 47. Yoon, Y. S., Seo, W. Y., Lee, M. W., Kim, S. T., and Koo, S. H. (2009) Salt-inducible kinase regulates hepatic lipogenesis by controlling SREBP-1c phosphorylation. *J. Biol. Chem.* **284**, 10446–10452
 48. Li, Y., Xu, S., Mihaylova, M. M., Zheng, B., Hou, X., Jiang, B., Park, O., Luo, Z., Lefai, E., Shyy, J. Y., Gao, B., Wierzbicki, M., Verbeuren, T. J., Shaw, R. J., Cohen, R. A., and Zang, M. (2011) AMPK phosphorylates and inhibits SREBP activity to attenuate hepatic steatosis and atherosclerosis in diet-induced insulin-resistant mice. *Cell Metab.* **13**, 376–388
 49. Goldstein, J. L., and Brown, M. S. (1990) Regulation of the mevalonate pathway. *Nature* **343**, 425–430
 50. Nagoshi, E., and Yoneda, Y. (2001) Dimerization of sterol regulatory element-binding protein 2 via the helix-loop-helix-leucine zipper domain is a prerequisite for its nuclear localization mediated by importin β . *Mol. Cell Biol.* **21**, 2779–2789
 51. Datta, S., and Osborne, T. F. (2005) Activation domains from both monomers contribute to transcriptional stimulation by sterol regulatory element-binding protein dimers. *J. Biol. Chem.* **280**, 3338–3345
 52. Magaña, M. M., and Osborne, T. F. (1996) Two tandem binding sites for sterol regulatory element binding proteins are required for sterol regulation of fatty-acid synthase promoter. *J. Biol. Chem.* **271**, 32689–32694
 53. Magaña, M. M., Koo, S. H., Towle, H. C., and Osborne, T. F. (2000) Different sterol regulatory element-binding protein-1 isoforms utilize distinct co-regulatory factors to activate the promoter for fatty acid synthase. *J. Biol. Chem.* **275**, 4726–4733
 54. Bennett, M. K., Seo, Y. K., Datta, S., Shin, D. J., and Osborne, T. F. (2008) Selective binding of sterol regulatory element-binding protein isoforms and co-regulatory proteins to promoters for lipid metabolic genes in liver. *J. Biol. Chem.* **283**, 15628–15637
 55. Lloyd, D. B., and Thompson, J. F. (1995) Transcriptional modulators affect *in vivo* protein binding to the low density lipoprotein receptor and 3-hydroxy-3-methylglutaryl coenzyme A reductase promoters. *J. Biol. Chem.* **270**, 25812–25818
 56. Pak, Y. K. (1996) Serum response element-like sequences of the human low density lipoprotein receptor promoter: possible regulation sites for sterol-independent transcriptional activation. *Biochem. Mol. Biol. Int.* **38**, 31–36
 57. Li, C., Kraemer, F. B., Ahlborn, T. E., and Liu, J. (1999) Induction of low density lipoprotein receptor (LDLR) transcription by oncostatin M is mediated by the extracellular signal-regulated kinase signaling pathway and the repeat 3 element of the LDLR promoter. *J. Biol. Chem.* **274**, 6747–6753
 58. Iizuka, K., and Horikawa, Y. (2008) ChREBP: a glucose-activated transcription factor involved in the development of metabolic syndrome. *Endocr. J.* **55**, 617–624
 59. Khoo, M. C., Oliveira, F. M., and Cheng, L. (2013) Understanding the metabolic syndrome: a modeling perspective. *IEEE Rev. Biomed. Eng.* **6**, 143–155
 60. Ni, Y. G., Wang, N., Cao, D. J., Sachan, N., Morris, D. J., Gerard, R. D., Kuro-O, M., Rothermel, B. A., and Hill, J. A. (2007) FoxO transcription factors activate Akt and attenuate insulin signaling in heart by inhibiting protein phosphatases. *Proc. Natl. Acad. Sci. U.S.A.* **104**, 20517–20522
 61. DeGrande, S. T., Little, S. C., Nixon, D. J., Wright, P., Snyder, J., Dun, W., Murphy, N., Kilic, A., Higgins, R., Binkley, P. F., Boyden, P. A., Carnes, C. A., Anderson, M. E., Hund, T. J., and Mohler, P. J. (2013) Molecular mechanisms underlying cardiac protein phosphatase 2A regulation in heart. *J. Biol. Chem.* **288**, 1032–1046
 62. Sablina, A. A., Hector, M., Colpaert, N., and Hahn, W. C. (2010) Identification of PP2A complexes and pathways involved in cell transformation. *Cancer Res.* **70**, 10474–10484
 63. Rodgers, J. T., Vogel, R. O., and Puigserver, P. (2011) Clk2 and B56 β mediate insulin-regulated assembly of the PP2A phosphatase holoenzyme complex on Akt. *Mol. Cell* **41**, 471–479
 64. Li, Y., Wei, H., Hsieh, T. C., and Pallas, D. C. (2008) Cdc55p-mediated E4orf4 growth inhibition in *Saccharomyces cerevisiae* is mediated only in part via the catalytic subunit of protein phosphatase 2A. *J. Virol.* **82**, 3612–3623
 65. Zhang, Z., Mui, M. Z., Chan, F., Roopchand, D. E., Marcellus, R. C., Blanchette, P., Li, S., Berghuis, A. M., and Branton, P. E. (2011) Genetic analysis of B55 α /Cdc55 protein phosphatase 2A subunits: association with the adenovirus E4orf4 protein. *J. Virol.* **85**, 286–295
 66. Mui, M. Z., Roopchand, D. E., Gentry, M. S., Hallberg, R. L., Vogel, J., and Branton, P. E. (2010) Adenovirus protein E4orf4 induces premature APC^{CCdc20} activation in *Saccharomyces cerevisiae* by a protein phosphatase 2A-dependent mechanism. *J. Virol.* **84**, 4798–4809